Eur Biophys J (2010) 39:1613–1623
DOI 10.1007/s00249-010-0619-6

ORIGINAL PAPER

Stability of Aβ (1-42) peptide fibrils as consequence of environmental modifications

Maria Gregori · Valeria Cassina · Doriano Brogioli · Domenico Salerno · Line De Kimpe · Wiep Scheper · Massimo Masserini · Francesco Mantegazza

Received: 21 April 2010 / Revised: 15 June 2010 / Accepted: 14 July 2010 / Published online: 9 August 2010

Abstract β-Amyloid peptide (Aβ) plays a key role in the pathogenesis of Alzheimer disease (AD). Monomeric Aβ undergoes aggregation, forming oligomers and fibrils, resulting in the deposition of plaques in the brain of AD patients. A widely used protocol for fibril formation in vitro is based on incubation of the peptide at low pH and ionic strength, which generates Aβ fibrils several microns long. What happens to such fibrils once they are brought to physiological pH and ionic strength for biological studies is not fully understood. In this investigation, we show that these changes strongly affect the morphology of fibrils, causing their fragmentation into smaller ones followed by their aggregation into disordered structures. We show that an increase in pH is responsible for fibril fragmentation, while increased ionic strength is responsible for the aggregation of fibril fragments. This behavior was confirmed on different batches of peptide either produced by the same company or of different origin. Similar aggregates of short fibrils are obtained when monomeric peptide is incubated under physiological conditions of pH and ionic strength, suggesting that fibril morphology is independent of the fibrillation protocol but depends on the final chemical environment. This was also confirmed by experiments with cell cultures showing that the toxicity of fibrils with different initial morphology is the same after addition to the medium. This information is of fundamental importance when Aβ fibrils are prepared in vitro at acidic pH and then diluted into physiological buffer for biological investigations.

Keywords Alzheimer disease · Amyloid · Protein aggregation · Dynamic light scattering · Atomic force microscopy

M. Gregori and V. Cassina contributed equally to this work.

M. Gregori (✉) · V. Cassina · D. Brogioli · D. Salerno · M. Masserini · F. Mantegazza
Department of Experimental Medicine,
University of Milano-Bicocca, via Cadore 48,
20052 Monza, MI, Italy
e-mail: m.gregori1@campus.unimib.it

L. De Kimpe · W. Scheper
Neurogenetics Laboratory, Academic Medical Center (AMC),
Meibergdreef 9, 1105 AZ Amsterdam, The Netherlands

Introduction

A prominent feature of Alzheimer's disease (AD)—a progressive neurodegenerative disease destroying memory and cognitive skills—is the extracellular accumulation in the brain of amyloid-beta (Aβ) (Irvine et al. 2008), a peptide derived from proteolytic cleavage of the transmembrane amyloid precursor protein (APP). Aβ is a small peptide of 39–42 amino acids that is formed and accumulates in anomalous amounts in AD by cleavage of APP (Selkoe 1999, 2004; LaFerla et al. 2007). When studied in vitro, Aβ monomers progressively aggregate, forming oligomers and fibrils that, when added to cultured neurons, induce oxidative stress, mitochondrial dysfunction, impaired synaptic transmission, disruption of membrane integrity, and impaired axonal transport. Such studies suggest an important role of Aβ in the progress of AD, even though Aβ deposition has not been correlated directly with neurodegeneration (Koo et al. 1999; Lorenzo and Yankner 1994; Weldon et al. 1998; Cazzaniga et al. 2007; Tabner et al. 2001).

The peptide composed of 42 amino acids (Aβ42) is more hydrophobic and more prone to fibril formation than others (Jarrett et al. 1993), and is also the predominant isoform found in cerebral plaques in AD (Findeis 2007). Current data have shown that soluble Aβ oligomers, also referred to

as Aβ-derived diffusible ligands (ADDLs), may play a key role in cytotoxicity (Chromy et al. 2003; Klein 2002; Bulbarelli et al. 2009a, b) inhibiting neuronal viability about 10-fold more than fibrils and about 40-fold more than unaggregated peptide (Dahlgren et al. 2002). The fibrillogenesis of Aβ42 has been investigated extensively by different techniques (Carrotta et al. 2005; Lomakin et al. 1996; Antzutkin 2004; Arimon et al. 2005; Harper et al. 1997; Parbhu et al. 2002), providing evidence that, upon incubation in vitro, distinct structural aggregates, including soluble oligomers, oligomeric globular aggregates, protofibrils, short fibrils, extended fibrils, and insoluble fibrillar aggregates, are formed successively (Yagi et al. 2007).

Since structural polymorphism is a prominent feature of Aβ aggregates both in vitro and in vivo (Petkova et al. 2005), different protocols have been developed to prepare the peptide in different aggregation forms as required for biological studies or to test the activity of candidate anti-amyloidogenic drugs. In a widely used protocol to prepare fibrillar Aβ, allowing reproducible aggregation kinetics (Lomakin et al. 1997), Aβ fibrillogenesis is developed at low pH, low ionic strength, and relatively high peptide concentration (Stine et al. 2003). Such a protocol offers important advantages: fibrillogenesis occurs much faster than at physiological pH and long, regular fibrils are formed. However, what happens to fibrillar structures prepared at low pH as a consequence of the changes of pH and ionic strength when they are diluted in physiological buffer, has never been investigated extensively.

In the present studies we used two complementary techniques, namely atomic force microscopy (AFM) and dynamic light scattering (DLS), to analyze the differences in the structure of Aβ42 fibrils formed at low pH and high Aβ concentration when they are subsequently diluted with buffer. AFM represents a powerful tool for the study of Aβ aggregation because it permits the visualization of biological macromolecules at the nanometric scale, while DLS provides ensemble statistical information.

In the following, we show that the modification of pH and ionic strength causes a dramatic, and very fast, fragmentation into small fibrils of the long fibrils previously prepared at low pH. In addition, we demonstrate that this modification is driven by the increase in pH rather than the change in ionic strength. Finally, a qualitative hypothesis to explain the origin of the observed effects is provided.

Materials and methods

Chemicals

Common chemicals, dimethyl sulfoxide (DMSO), 1,1,1,3,3,3-hexafluoro-2-propanol (HFIP) and Thioflavin T (ThT) were purchased from Sigma-Aldrich (St. Louis, MO). All cell cultures reagents were purchased from Invitrogen (Carlsbad, CA). LIVE/DEAD® Cell Viability assay was purchased from Molecular Probes (Eugene, OR).

Fibril forming conditions and dilution

Three different batches of Aβ (1-42) peptide were purchased from Sigma-Aldrich; within this investigation, these will be referred to as batch A, B or C. In addition, we received a generous gift of a synthetic Aβ (1-42) peptide with controlled purity of 90–95% obtained as described (Manzoni et al. 2009) from M. Salmona (Mario Negri Institute for Pharmacological Research, Milan, Italy). Pre-existing Aβ aggregates were disintegrated into monomers, dissolving the peptide in HFIP at 1 mg/ml concentration, and then aliquoted in Eppendorf tubes.

To prepare fibrils at acidic pH, the procedure described by Dahlgren et al. (2002) was followed. Briefly, aliquots of Aβ dissolved in HFIP were allowed to evaporate, dried under vacuum, and the peptides was dissolved at 5 mM concentration in DMSO. Then, a volume of 10 mM HCl sufficient to bring the peptide to 100 μM concentration was added. The peptide solution was incubated for 24 h at 37°C in a screw-capped vial (in order to avoid the loss of HCl) was taken as the sample of fibrils obtained at acidic pH.

Fibrils obtained as described above were then diluted to 20 μM or 3 μM with: (1) 10 mM Tris/HCl pH 7.4, 150 mM NaCl (Tris-buffered saline), (2) 150 mM NaCl in 10 mM HCl, or (3) 10 mM Tris/HCl pH 7.4 (Tris buffer).

Alternatively, the procedure described by Liu et al. (2005) to obtain fibrils directly in buffer was followed. Briefly, aliquots of Aβ dissolved in HFIP were allowed to evaporate and dried under vacuum. The peptide was dissolved to a concentration of 220 μM in DMSO and diluted to 20 μM in 10 mM Tris HCl, 150 mM NaCl, pH 7.4 (Tris-buffered saline) and then incubated at 37°C for 24 h. The morphology of the resulting fibrils was checked by AFM and DLS. During all stages of sample preparation we took care not to shake the solution in order to minimize fibril breakage on mixing the solution. All experiments were replicated three times using different batches of peptide produced by the same company and batches of different origin.

Atomic force microscopy

The data presented here were acquired with a Nanowizard II (JPK Instruments, Berlin, Germany), with the overlay option, which allows a direct view of the sample and the cantilever on the same image. In this set up, the AFM head is placed on a Zeiss optical microscope and image acquisition and analysis is performed using JPKs software. The measurements were performed in Tapping Mode in air

using stiff silicon cantilevers (RTESP-Veeco, resonant frequencies ~300 kHz, spring constant ~40 N/m). AFM images were acquired at a scan rate of 1 Hz.

For the AFM measurements, 10 µl of sample solution is deposited on an atomically flat surface (freshly cleaved mica, Ted Pella, Redding, CA). The sample was incubated at room temperature for 5 min to steadily adsorb to the mica surface, then rinsed with distilled water to minimize change in local ionic strength during drying, and water dried under gentle nitrogen flow (Dahlgren et al. 2002; Stine et al. 2003; Yagi et al. 2007).

Dynamic light scattering

DLS provides a fast, simple, and non-invasive method of evaluating the average size of nano and micro particles dispersed in transparent solvent, and thus for characterizing particle aggregation. Here, we present DLS measurements performed using a Brookhaven 90Plus system (Brookhaven Instruments, http://www.bic.com/). In this apparatus, a $\lambda = 652$ nm diode laser is focused via an optical fiber onto a sample positioned in a 50 µl standard cell, and the scattered light is collected by an avalanche photodiode at $\alpha = 90°$. From the statistical analysis of the intensity fluctuations measured by the photodiode, an average hydrodynamic radius, R_H, of the suspended particles is obtained. In our situation the problem is more intricate since we are in the presence of flexible linear objects (amyloid fibrils) of different lengths (polydisperse). Flexible linear objects are usually characterized by a total contour length L_t (total length measured along the chain), and a persistence length L_p (minimum average distance along which it is possible to consider the chain straight). For polydisperse particles or aggregates, the statistical distribution of particle size can be obtained by using standard CONTIN or cumulant methods (Pecora 1985; Chen et al. 1981). Here we present data collected with a CONTIN algorithm where, by comparing the measured correlation function and the mono-exponential function, we obtain an evaluation of the different size populations in the solution. The histograms obtained show the size distribution of the aggregates, and allow evaluation of the average aggregate dimension, whether the system is mono or polydisperse, and the width of the distribution.

The DLS and AFM techniques are complementary for the following reasons. DLS is an intrinsically ensemble technique since it measures the scattering of several objects simultaneously, and allows easy statistics. For this reason, DLS can give us information about the details of the polydispersity of the sample, even given the important drawback that the scattered intensity is weighted by the scattering signal of the various particles. The signal due to the small particles is lower with respect to the signal due to the bigger particles. On the other hand, AFM is aimed at imaging on single nano objects, and thus some statistical analysis may be required after measurements. This is particularly important when the system is polydisperse since, in this case, the AFM field of view could overestimate the presence of diffuse small aggregates with respect to the occurrence of rare large objects.

Thioflavin T fluorescence assay

The extent of Aβ (1-42) peptide aggregation was followed by withdrawing aliquots from the samples of fibrils prepared at acidic pH, and of the same fibrils previously diluted to 20 µM in Tris-buffered saline and incubated for 90 min or for 24 h. The samples were added to 10 µM Thioflavin T (ThT) as described (Taylor et al. 2010) to give a final Aβ (1-42) concentration of 5 µM. Fluorescence intensity was monitored using an excitation wavelength of 450 nm and an emission wavelength of 482 nm. Experiments were carried out in triplicate using different batches of peptide produced by the same company and of different origin.

Cell culture and toxicity assays

To test the possible influence of the aggregation protocol on peptide cytotoxicity, experiments were carried out on cultured human neuroblastoma cells (SK-N-SH) after differentiation with retinoic acid, as described (Chafekar et al. 2007). Samples were added to the cell culture at 2 µM final peptide concentration. Toxicity was evaluated in six replicates after 24 h at 37°C, using two different neurotoxicity assays, namely MTT and ethidium homodimer-1 (EthD-1) incorporation assay. Untreated cells or cells treated with 2 µM Thapsigargin (TG) (Sigma) were used as controls. For the MTT assay, a protocol described elsewhere was used (Chafekar et al. 2007). For EthD-1 incorporation assay, the LIVE/DEAD® Cell Viability (Molecular probes) assay was used according to the manufacturer's protocol. The fluorescent signal was measured in a Fluostar Omega microplate reader.

Results and discussion

While the parameters affecting the Aβ peptide aggregation process have been investigated extensively and mostly clarified (Zagorski et al. 1999; Lee et al. 2007; Kusumoto et al. 1998; Ahmad et al. 2009), how environmental conditions influence the morphology of pre-formed fibrils is not yet completely understood. The aim of this work was to investigate the influence of pH and/or ionic strength on Aβ (1-42) peptide fibril structure.

Analysis was performed in parallel using AFM and DLS techniques. For all experimental conditions tested, the

results obtained with AFM and DLS were highly reproducible. Herein, we show some representative AFM images that provide direct visual information on the deposited fibril morphology, and DLS data providing histograms of the statistical size distribution of these objects in solution.

Effect on fibrils prepared at acidic pH of dilution in Tris-buffered saline

The starting point of our investigation is a system of fibrils obtained via a standard protocol performed at low pH (pH 2), namely by incubation of 100 μM Aβ 1-42 in 10 mM HCl, at 37°C for 24 h (Dahlgren et al. 2002; Stine et al. 2003). For these experiments, all Aβ peptides utilized in the present study were tested (i.e. those from Mario Negri and from Sigma, batch A, B and C). As shown by the AFM images in Fig. 1a, as already reported in literature, the chains appear unbranched, slightly curved, and several microns long. Such long fibrils exhibit an apparent height of 6 nm, but this value could be slightly underestimated because of sample compression due to the AFM probe (Harper et al. 1997). The DLS experiments presented in Fig 1b show that these structures have an average hydrodynamic radius of about 100 nm. This figure is compatible with the hydrodynamic radius of a flexible chain with the morphological characteristics (total length L_t and persistence length L_p) measured by AFM. This is confirmed by Fig. 2, in which we have plotted the theoretical value of the hydrodynamic radius, R_H, of a flexible chain of fixed L_t and L_p as a function of L_t, calculated as described by Harnau et al. (1996), for three different values of persistence length (L_p = 50, 200, 500 nm).

The Aβ fibrils obtained at acidic pH were diluted successively from the original concentration of 100 μM in HCl, to a final concentration of 20 μM in Tris-buffered saline, since these conditions are those typically utilized for biological experiments (see, for instance, Patel et al. 2006; Talmard et al. 2007; Lin et al. 2007). Diluted Aβ was maintained at room temperature and analyzed by AFM after 30 and 90 min (Fig. 1c, e) and by DLS after 30, 90 min and 24 h (Fig. 1d, f, g). AFM observations at 30 min after dilution (Fig. 1c) show disordered small aggregates constituted by fibrils fragments. DLS data (Fig. 1d) confirm AFM results, showing an increase in the hydrodynamic radius, compatible with the appearance of aggregates. The fragmentation phenomenon continues with time and, after 90 min, only short fibrils, ranging from 100 to 300 nm, are present (Fig. 1e). In the same image it is possible to notice the presence of dots; however, it is not possible to precisely resolve the nature of these dots because the convolution between tip and sample hides their small features and elongation. DLS data taken on the same system (Fig. 1f) at 90 min detect only the presence of large aggregates (>1 μm). After longer incubation, the aggregate size appears even larger, as shown in Fig. 1g, suggesting a progressive aggregation process. In parallel, the majority of AFM fields do not display any structures (data not shown). As shown by the above results obtained after dilution in buffer, the elongated fibril structure is not stable, and undergoes a rapid decrease in average length, followed by a slow aggregation of the resulting short fibrils. In the case of aggregates, shown in Fig. 1f,g, the hydrodynamic radius measured by DLS represents the radius of the aggregate. In this case, we did not use the flexible chain model since we were not observing single, separated, unbranched fibril as in Fig. 1a.

The same effects, fibril fragmentation followed by aggregation, was detected by diluting Aβ at 3 μM final concentration with Tris-buffered saline (data not shown), another buffer widely used for biological in vitro studies (Choucair et al. 2007).

The behavior of the peptide described above was reproduced using different batches of Aβ and peptides of different source. These observations are particularly relevant, because in several experiments in vitro (see for instance Bravo et al. 2008; Moretto et al. 2007; Yan et al. 2006), the dilution in physiological buffer of fibrils obtained in HCl is assumed to have no effect on their morphology. Of course the importance of this information is methodological, since the conditions adopted for fibril formation in vitro (pH 2 and high protein concentrations) do not apply in vivo.

Comparison between AFM and DLS data deserves some comment. Figure 1a and b suggest that the two techniques identify objects of the same size. On the contrary, Fig. 1e and f apparently show that AFM and DLS are aiming at objects of different size although referring to the same sample. This fact is due to the essential features of the two techniques, and in particular to their different sensitivity range (see Materials and methods). Indeed, the AFM image presented in Fig 1e shows the residual fibril fragments resulting after dilution, while the DLS data of Fig. 1f and g detect the presence in solution of aggregates constituted by those fragments. The very large structures detected by DLS are not easily identified in the AFM field of view, while the small objects imaged by AFM are not detectable in DLS measurements, since their scattering signal is covered by the comparatively large signal of the bigger objects. These data confirm the complementarities of AFM and DLS data in an experimental situation where the size of the objects under investigation is extremely polydisperse. This interpretation is confirmed by an accurate inspection of AFM images, which depict average fields: as matter of fact, it is possible to observe a lower amount of Aβ on the mica surface in Fig. 1e taken 90 min after dilution, in comparison with Fig. 1a and c, taken before or immediately after dilution. This lower amount of Aβ is compatible with the presence of large fibrillar aggregates with an average size of the

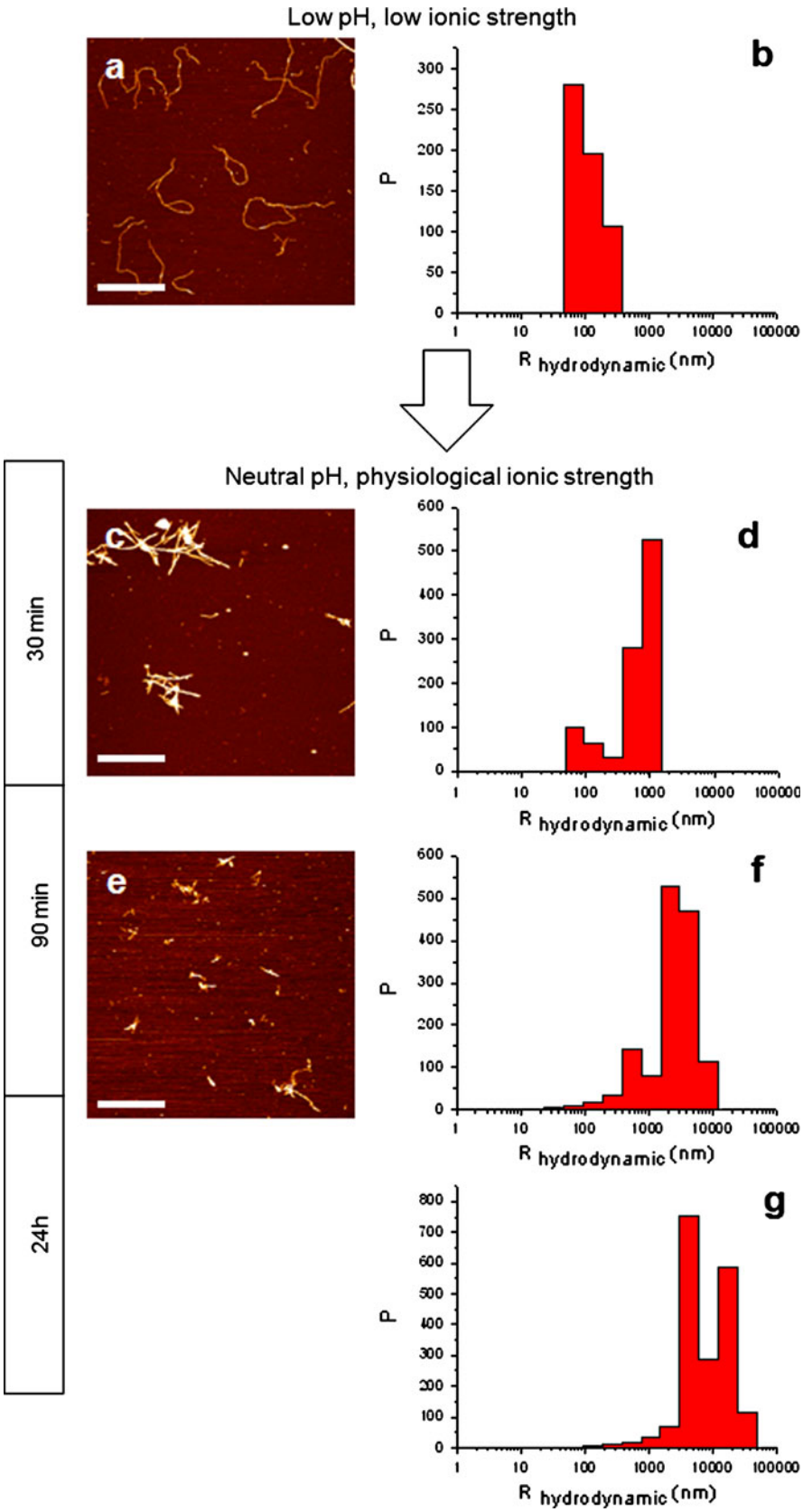

Fig. 1 Morphology of HCl β-amyloid peptide (Aβ) (1-42) fibrils before (**a**, **b**) and after dilution in Tris-buffered saline (**c**–**f**). **a**, **c**, **d** Atomic force microscopy (AFM) images of 4×4 µm x–y, 6 nm total z-range. *Bar* 1 µm. **b**, **e**, **f** Histograms of hydrodynamic radius, R_H, distribution as obtained by dynamic light scattering (DLS) measurements. *Vertical left bar* Measurement times after dilution in Tris-buffered saline. The examples shown refer to Aβ1-42 from Sigma, batch A

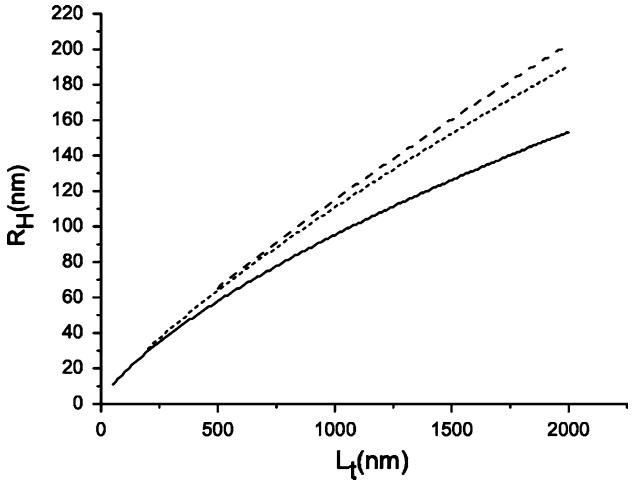

Fig. 2 Theoretical hydrodynamic radius R_H of a flexible chain of total contour length L_t and persistence length L_p plotted as a function of L_t for three different values of L_p. See text for details. *Continuous line* $L_p = 50$ nm, *dotted line* $L_p = 200$ nm, *dashed line* $L_p = 500$ nm

order of several microns, detected by DLS (Fig. 1f, g). Such large fibrillar aggregates are statistically very rare on the mica surface, and so almost undetectable by AFM scanning, which can explore only a restricted area.

ThT fluorescence emission experiments were carried out with fibrils formed in acidic conditions, before and after dilution in Tris-buffered saline in order to detect the possible formation of new fibrils as a consequence of the increase in pH and salt concentration. No differences were found in the ThT fluorescence emission intensity before (31,063 ± 0.386 A.U.), 90 min (31,466 ± 0.127 A.U.) and 24 h (30,075 ± 0.467 A.U.) after dilution, suggesting that the environmental change induces a morphological alteration of fibrils that were already present in solution, without the apparent formation of new ones.

Changes in ionic strength or pH affect the structure of fibrils obtained at acidic pH differently

In order to further investigate the factors critical controlling fragmentation/aggregation of Aβ fibrils obtained in HCl once they are diluted in buffer, we studied the effects on fibrils morphology of ionic strength and of pH change separately. For these experiments, all Aβ peptides utilized in the present study were tested (from Mario Negri and from Sigma, batch A, B and C).

Again, the starting point is long unbranched fibrils obtained at low pH. Their dilution in 150 mM NaCl, maintaining the pH at 2.0, does not affect their structure (Fig. 3a, b). Indeed, the total length and the persistence length, as estimated qualitatively by AFM, and the distribution of the hydrodynamic radii, as evaluated from DLS, are comparable before (Fig. 1a, b) and 90 min after salt addition (Fig. 3a, b).

We next evaluated the effect of increasing the pH from acidic conditions to 7.4 without increasing the ionic strength. In this case we observed, after 90 min, a fragmentation of the long fibrils (Fig. 3c, d) into shorter ones of about 100–300 nm in length, without formation of aggregates. As suggested from both AFM and DLS experiments (Fig. 3c, d), the average hydrodynamic radius is critically decreased to an average size of about 30 nm. It is worth noting that, in this case, the DLS radius distribution appears monodisperse, presumably because, given the DLS sensitivity, the small length polydispersity visible from the AFM images is not enough to induce a significant polydispersity in the measured DLS size distribution. Light scattering data are more sensitive to big objects, thus the very low concentration of big structures, as in the present polydisperse case, is a particularly favorable condition because it allows direct comparison of the fibril size obtained with the two techniques (Fig. 3c, d), in analogy to the case shown in Fig. 1a, b.

Finally, the short fibrils obtained as described above by changing the pH from 2 to 7.4, were mixed with a the quantity of NaCl required to give a final concentration of 150 mM NaCl. This change in ionic strength induces the formation of disordered aggregates (data not shown), in analogy to what we observed when the pH and the ionic strength were changed simultaneously by the addition of Tris-buffered saline (Fig. 1e, f).

The three sets of experiments allowed us to identify the origin of the morphological changes observed on fibrils prepared in HCl and then diluted in Tris-buffered saline. Indeed, the results show that the increase in pH is responsible for inducing fibril fragmentation, while the increase in ionic strength is responsible for the aggregation of fibril fragments.

Fibril morphology: final chemical conditions vs fibrillation history

Finally, we studied the historical dependence of the fibril structure, with the aim of answering the following question: does the final fibril structure depend on the final chemical environment (solvent composition, pH, ionic strength, Aβ concentration) or also on the history passed through to reach that final chemical environment?

With this aim, we compared the morphology of Aβ fibrils under the same final conditions (namely: Tris-buffered saline, Aβ concentration 20 μM) but arrived at via two different ways: in the first, Aβ fibrils were formed at low pH and then diluted with Tris-buffered saline (Fig. 1e, f). In the second, Aβ was incubated directly in Tris-buffered saline at 37°C for 24 h (Fig. 4a, b). In this latter case, the DLS histogram (Fig 4b) shows a bi-disperse system constituted by objects with hydrodynamic

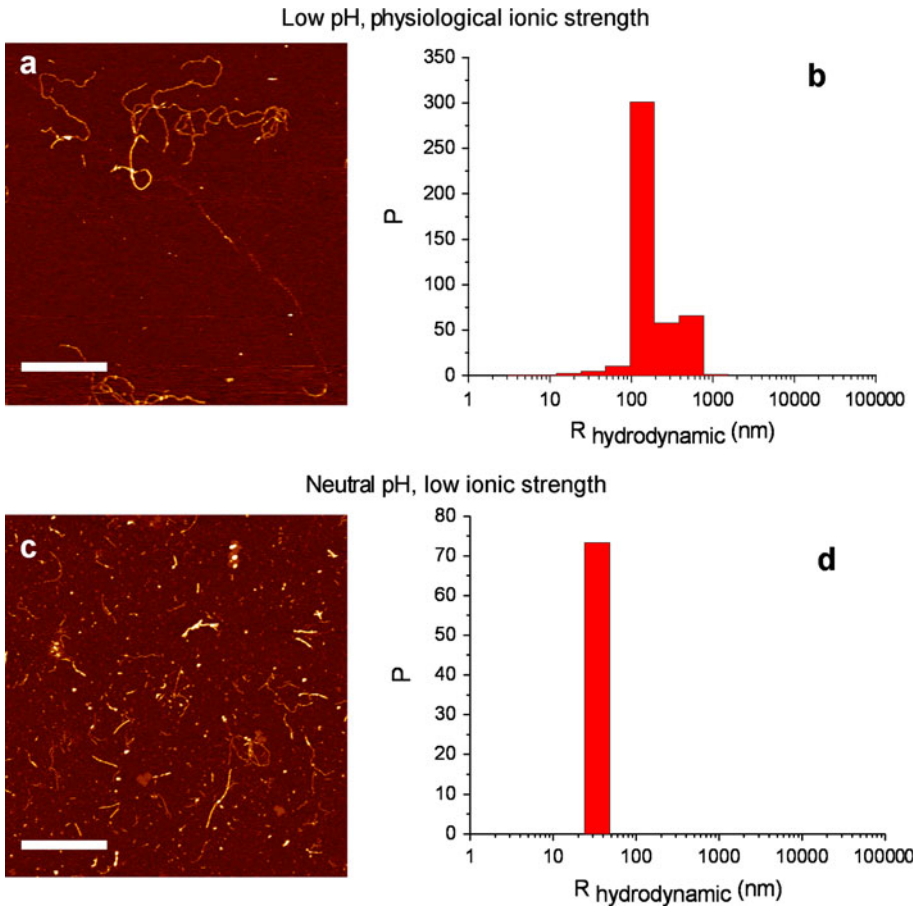

Fig. 3 Morphology of HCl Aβ (1-42) fibrils obtained 90 min after dilution at various values of pH and ionic strength. **a**, **c** AFM images of 4 × 4 μm *x*–*y*, 6 nm total *z*-range. *Bar* 1 μm. **b**, **d** Histograms of hydrodynamic radius, R_H, distribution as obtained by DLS measurements. Data in **a** and **b** were obtained after addition of 150 mM NaCl, pH 2. Data in **c** and **d** were obtained after dilution in Tris buffer, pH 7.4. The examples shown refer to Aβ1-42 from Sigma, batch A

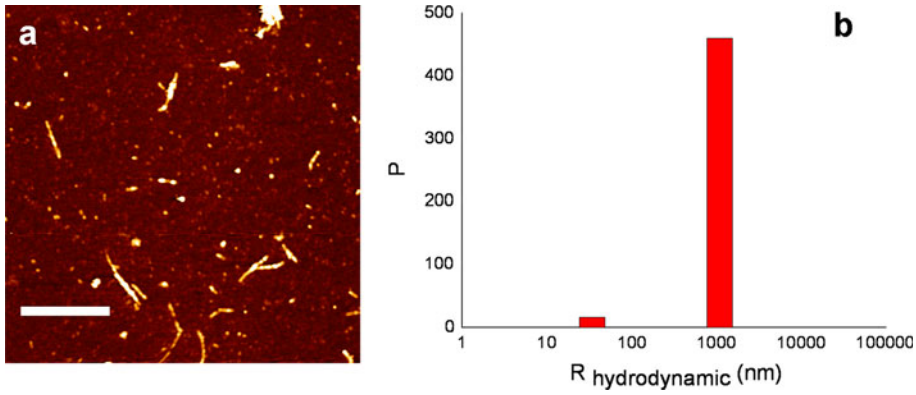

Fig. 4 Morphology of Aβ (1-42) fibrils formed after 24 h of incubation in Tris-buffered saline. **a** AFM image of 4 × 4 μm *x*–*y*, 6 nm total *z*-range. *Bar* 1 μm. **b** Histograms of hydrodynamic radius R_H distribution as obtained by DLS measurements. The examples shown refer to Aβ1-42 from Sigma, batch B

radii of about 50 and 1 μm. It is important to stress that the frequencies of occurrence of the two distinct peaks at 50 nm and 1 μm appear very different. In this context, we recall again that the DLS histograms reported in this paper are weighted by considering the scattering signal, which depends approximately on the square of the particle volume. The small peak at 50 nm corresponds to a low percentage of the small particle volume, but to a large percentage of the small particle number. DLS experiments and AFM images show that both protocols lead to the formation of very similar structures, that is, a mixture of separated short fibrils and larger aggregates of short fibrils. Scanning the samples by AFM carefully, it was possible to detect large aggregates of small fibrils (Fig. 5). For these experiments, Aβ peptides from Sigma were tested (batch A, B and C).

Overall, these experiments clearly indicate that the same fibril morphology depends on the final environment in which fibrils are placed, independent of the preceding fibrillation history.

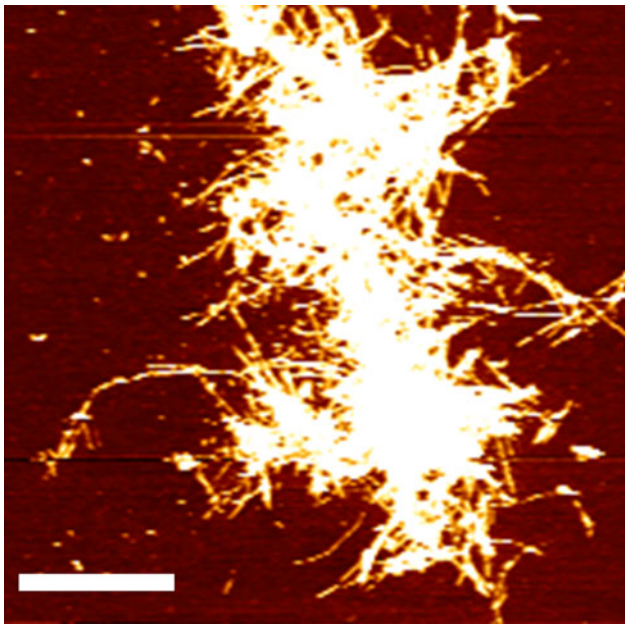

Fig. 5 Image of a large aggregate of small fibrils, formed after 24 h of incubation of Aβ (1-42) monomers in Tris-buffered saline. AFM image, 4 × 4 µm *x*–*y*, 6 nm total *z*-range. *Bar* 1 µm. The example shown refer to Aβ1-42 from Sigma, batch B

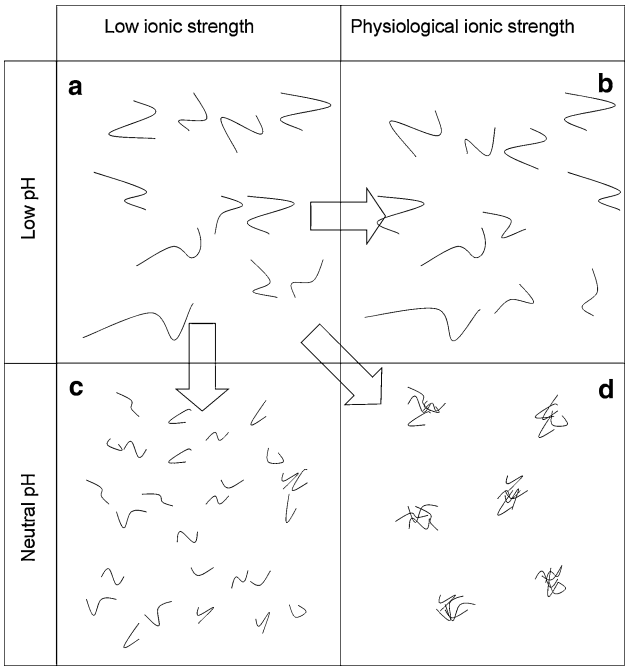

Fig. 6 Qualitative sketch of morphological characteristics of HCl Aβ (1-42) fibrils before (**a**) and after dilution in various chemical environments (**b**, **c**, **d**)

These observations are resumed in the sketch shown in Fig. 6, where we show schematically the Aβ fibrils morphology resulting from the experiments performed. Rows and columns of the table indicate the various values of pH and ionic strength, while the arrows correspondingly specify the variation of the chemical environment.

Cytotoxicity of differently aggregated Aβ fibrils

Long fibrils formed at pH 2 (depicted in Fig. 1a) and large aggregates of short fibrils (as depicted in Fig. 4), showed comparable toxicity when added to the cell cultures (Fig. 7), as evaluated both by MTT and by EthD-1 incorporation assay (87 and 90% cell survival, respectively). This result may be interpreted as a consequence of the observation, considering the present investigation, that fibril morphology depends on the final environment and not on the fibrillation history of the sample. However, as shown above, the sample of fibrils formed at pH 2 is fragmented and aggregates after 90 min in physiological buffer, becoming indistinguishable from the other sample; therefore, the difference between the two samples is limited in time and may affect the results observed. Possibly, a separate investigation would be necessary to explore this issue.

Qualitative modeling

In order to provide a theoretical framework capable of justifying the observed phenomena qualitatively, we consider the Aβ fibrils resulting from aggregation of elementary protofibrils, as reported in the literature (Arimon et al. 2005). Such an aggregation process can give rise to fibrils of different length (Fig. 6a–c) or to disordered aggregates of short fibrils (Fig. 6d). The main object of a theory explaining the obtained different structures of Aβ aggregates is then to clarify the molecular origin of the various chemical interactions giving rise to the resulting structures in various chemical environments. The formation of protofibrils from Aβ monomers has been investigated extensively and can be modeled with ab initio calculations (Luhrs et al. 2005; Protein Data Bank, code 2BEG, http://www.rcsb.org/pdb/explore/explore.do?structureId=2BEG). On the contrary, protofibril aggregation giving rise to fibrils is still poorly understood. Unfortunately, the system is too complex to perform any useful ab initio molecular dynamics calculation. Thus, a simplification of the model is required, and we show here the key features required in order to describe the phenomena observed.

The starting point is the Aβ protofibril model shown schematically, not to scale, in Fig. 8 for two different pH values. As illustrated in the picture, the protofibrils are described as aggregates of stacked Aβ monomers (indicated as small parallepipeds with a hair), linked by cross-beta hydrogen bonds, with the β-sheet plane perpendicular to the protofibril axis. The resulting protofibril made of this assembly of small parallepipeds has a roughly rectangular section of 1 × 2 nm (Luhrs et al. 2005; Protein Data Bank, code 2BEG) composed by aminoacids 17-42 (protofibril body), while aminoacids 1-16 constitute disordered tails (protofibril hair). The protofibril is twisted around its axis,

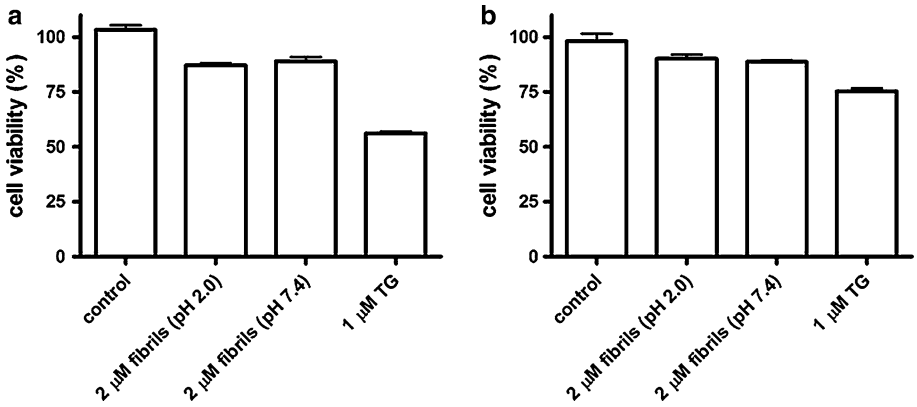

Fig. 7 **a** Differentiated SK-N-SH were treated with 2 μM Aβ fibrils or with 1 μM TG for 24 h. Cell viability was measured using an MTT assay and is depicted as a percentage of the untreated cells (*control*). **b** Differentiated SK-N-SH were treated with 2 μM Aβ fibrils or with 1 μM TG for 24 h. Cell viability was determined with an ethidium homodimer-1 (EthD-1) incorporation assay and is depicted as a percentage of the untreated cells (*control*). *Columns* Mean ± S.E.M ($n = 6$) from one experiment; the results shown are representative of three independent experiments

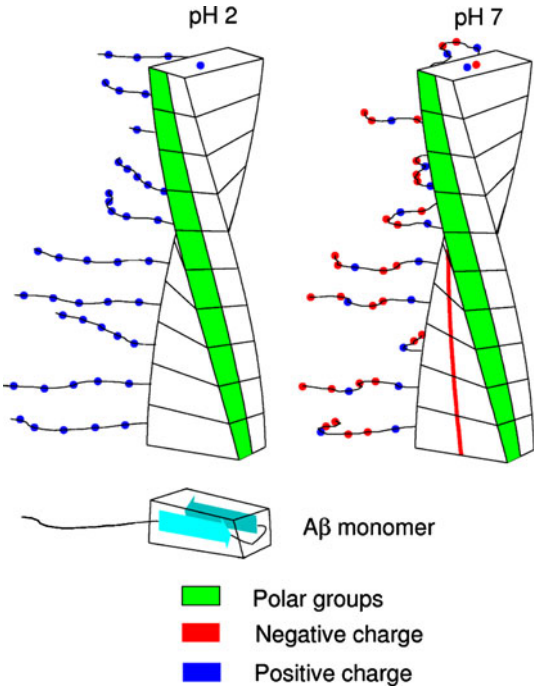

Fig. 8 Qualitative sketch (not to scale) of Aβ protofibril structure at different pH values

with a helical pitch of about 100 nm (Protein Data Bank). It is well known that fibrils are created by aggregation of protofibrils, which are assembled and twisted around one another (Makin and Serpell 2005). From the molecular structure, we can notice that the protofibril body exposes mainly hydrophobic aminoacids. Polar groups are present only on a small part of the surface (green stripe in Fig. 8), corresponding to Ser 26 and Asn 27. At pH 7.4, a negative charge on the side of the body is also present (red stripe in Fig. 8), due to the carboxylic residue of Glu 22. The most charged region of the protofibril is due to the Aβ tails composed by amino acids 1–16: at pH 2 it contains five positive charges, and at pH 7.4 it contain four negative charges and two positive charges. Other charges are buried inside the protofibril body, and do not contribute to electrostatic effects due to Debye shielding. Fibril formation can be seen as the aggregation of protofibrils through the sticking of the lateral surfaces, due to hydrophobic interaction among protofibril bodies (side–side aggregation), leaving the charged and hydrophilic tails outside. This kind of aggregation is favored at pH 2, since there is no charge on the protofibril body surface. It is well known that, in analogy with our system, this kind of lateral aggregation leads eventually to elongated structures, as described for other classical biochemical systems. e.g., fibrin (Sicorello et al. 2009), collagen (Yang and Kaufman 2009), lysozyme (Hill et al. 2009), and insulin (Zako et al. 2009).

On the other hand, at pH 7.4, the glutamic acid exposes its negative charge (red stripe in Fig. 8). In this situation, these charges on the protofibril body surface prevent the hydrophobic lateral interaction, thus leading to fragmentation of already assembled fibrils, or avoiding the formation of elongated structures, as described above. Therefore, at low pH values, the hydrophobic interaction induces an anisotropic elongation of the aggregates, while at physiological pH the presence of exposed charges, partially disturbing the hydrophobic interaction, allows the isotropic aggregation.

Finally, the aggregation of protofibrils induced by increasing the ionic strength at pH 7.4, under conditions of reduced hydrophobic interaction, can be explained qualitatively within the frame of DLVO (Derjaguin-Landau-Verwey-Overbeek) theory, similarly to what has already been reported about well described colloidal aggregation phenomena (Russel et al. 1989; Olsen et al. 2009). Accordingly, the increase in ionic strength induces an aggregation

of protofibrils, since the electric charge is too screened to ensure adequate particle repulsion (Sahoo et al. 2009). The effect of ionic strength is not relevant at pH 2, where the charge screening is not enough to overcome the hydrophobic interaction.

Conclusions

Our results highlight the critical role played by pH and ionic strength in Aβ fibrils morphology. Moreover, our data show that the chemical environment continues to exert a great influence even after the completion of fully grown Aβ fibrils, suggesting that their structure is not static, but prone to morphological modification. The features of Aβ fibrillation have been studied extensively but differences in structure in different solvents have usually been attributed to different rates of fibril growth (Shen and Murphy 1995). Here, we provide evidence that fibrils morphology in a defined solvent is independent of the fibrillation protocol but depends on the final chemical environment. This analysis is of fundamental importance when Aβ fibrils are diluted into physiological buffer for biological investigations.

Acknowledgments The research leading to these results has received funding from the European Community's Seventh Framework Programme (FP7/2007–2013) under grant agreement no 212043.

References

Ahmad A, Muzaffar M, Ingram VM (2009) Ca^{2+}, within the physiological concentrations, selectively accelerates Aβ42 fibril formation and not Aβ40 in vitro. Biochim Biophys Acta 1794:1537–1548

Antzutkin ON (2004) Amyloidosis of Alzheimer's Aβ peptides: solid-state nuclear magnetic resonance, electron paramagnetic resonance, transmission electron microscopy, scanning transmission electron microscopy and atomic force microscopy studies. Magn Reson Chem 42:231–246

Arimon M, Díez-Pérez I, Kogan MJ, Durany N, Giralt E et al (2005) Fine structure study of Aβ1-42 fibrillogenesis with atomic force microscopy. FASEB J 19:1344–1346

Bravo R, Arimon M, Valle-Delgado JJ, García R, Durany N et al (2008) Sulfated polysaccharides promote the assembly of amyloid β1-42 peptide into stable fibrils of reduced cytotoxicity. J Biol Chem 283:32471–32483

Bulbarelli A, Lonati E, Cazzaniga E, Gregori M, Masserini M (2009a) Pin1 affects Tau phosphorylation in response to Aβ oligomers. Mol Cell Neurosci 42:75–80

Bulbarelli A, Lonati E, Cazzaniga E, Re F, Sesana S, Barisani D, Sancini G, Mutoh T, Masserini M (2009b) TrkA pathway activation induced by amyloid-beta (Abeta). Mol Cell Neurosci 40:365–373

Carrotta R, Manno M, Bulone D, Martorana V, San Biagio PL (2005) Protofibril formation of amyloid β-protein at Low pH via a non-cooperative elongation mechanism. J Biol Chem 280:30001–30008

Cazzaniga E, Bulbarelli A, Cassetti A, Lonati E, Re F, Palestini P, Mutoh T, Masserini M (2007) β-Amyloid (25–35) enhances lipid metabolism and protein ubiquitination in cultured neurons. J Neurosci Res 85:2253–2261

Chafekar SM, Hoozemans JJ, Zwart R, Baas F, Scheper W (2007) Abeta 1-42 induces mild endoplasmic reticulum stress in an aggregation state-dependent manner. Antioxid Redox Signal 9:2245–2254

Chen S-H, Chu B, Nossal R (1981) Scattering techniques applied to supramolecular and non equilibrium systems. Plenum, New York

Choucair A, Chakrapani M, Chakravarthy B, Katsaras J, Johnston LJ (2007) Preferential accumulation of Aβ (1-42) on gel phase domains of lipid bilayers: an AFM and fluorescence study. Biochim Biophys Acta 1768:146–154

Chromy BA, Nowak RJ, Lambert MP, Viola KL, Chang L et al (2003) Self-Assembly of Aβ1-42 into globular neurotoxins. Biochemistry 42:12749–12760

Dahlgren KN, Manelli AM, Stine WB Jr, Baker LK, Krafft GA, LaDu MJ (2002) Oligomeric and fibrillar species of amyloid-β peptides differentially affect neuronal viability. J Biol Chem 277:32046–32053

Findeis MA (2007) The role of amyloid β peptide 42 in Alzheimer's disease. Pharmacol Therapeut 116:266–286

Harnau L, Winkler RG, Reineker P (1996) Dynamic structure factor of semiflexible macromolecules in dilute solution. J Chem Phys 104:6355–6368

Harper JD, Wong SS, Lieber CM, Lansbury PT Jr (1997) Observation of metastable Aβ amyloid protofibrils by atomic force microscopy. Chem Biol 4:119–125

Hill SE, Robinson J, Matthews G, Muschol M (2009) Amyloid protofibrils of lysozyme nucleate and grow via oligomer fusion. Biophys J 96:3781–3790

Irvine GB, El-Agnaf OM, Shankar GM, Walsh DM (2008) Protein aggregation in the brain: the molecular basis for Alzheimer's and Parkinson's diseases. Mol Med 14:451–464

Jarrett JT, Berger EP, Lansbury PT Jr (1993) The carboxy terminus of the amyloid protein is critical for the seeding of amyloid formation: implications for the pathogenesis of Alzheimer's disease. Biochemistry 32:4693–4697

Klein WL (2002) Aβ toxicity in Alzheimer's disease: globular oligomers (ADDLs) as new vaccine and drug targets. Neurochem Int 41:345–352

Koo EH, Lansbury PT Jr, Kelly JW (1999) Amyloid diseases: abnormal protein aggregation in neurodegeneration. Proc Natl Acad Sci USA 96:9989–9990

Kusumoto Y, Lomakin A, Teplow DB, Benedek GB (1998) Temperature dependence of amyloid β-protein fibrillization. Proc Natl Acad Sci USA 95:12277–12282

LaFerla FM, Green KN, Oddo S (2007) Intracellular amyloid- in Alzheimer's disease. Nat Rev Neurosci 8:499–509

Lee S, Fernandez EJ, Good TA (2007) Role of aggregation conditions in structure, stability, and toxicity of intermediates in the Aβ fibril formation pathway. Protein Sci 16:723–732

Lin M-S, Chiu H-M, Fan F-J, Tsai H-T, Wang SS-S et al (2007) Kinetics and enthalpy measurements of interaction between β-amyloid and liposomes by surface plasmon resonance and isothermal titration microcalorimetry. Colloid Surface B 58:231–236

Liu R, Barkhordarian H, Emadi S, Park CB, Sierks MR (2005) Trehalose differentially inhibits aggregation and neurotoxicity of beta-amyloid 40 and 42. Neurobiol Dis 20:74–81

Lomakin A, Chung DS, Benedek GB, Kirschner DA, Teplow DB (1996) On the nucleation and growth of amyloid β-protein fibrils: detection of nuclei and quantitation of rate constants. Proc Natl Acad Sci USA 93:1125–1129

Lomakin A, Teplow DB, Kirschner DA, Benedek GB (1997) Kinetic theory of fibrillogenesis of amyloid β-protein. Proc Natl Acad Sci USA 94:7942–7947

Lorenzo A, Yankner BA (1994) β-Amyloid neurotoxicity requires fibril formation and is inhibited by Congo red. Proc Natl Acad Sci USA 91:12243–12247

Luhrs T, Ritter C, Adrian M, Riek-Loher D, Bohrmann B et al (2005) 3D structure of Alzheimer's amyloid-beta (1-42) fibrils. Proc Natl Acad Sci USA 102:17342–17347

Makin OS, Serpell LC (2005) Structures for amyloid fibrils. FEBS J 272:5950–5961

Manzoni C, Colombo L, Messa M, Cagnotto A, Cantù A, Del Favero E, Salmona M (2009) Overcoming synthetic Aβ peptide aging: a new approach to an age-old problem. Amyloid 16:71–80

Moretto N, Bolchi A, Rivetti C, Imbimbo BP, Villetti G et al (2007) Conformation-sensitive antibodies against Alzheimer amyloid-β by immunization with a thioredoxin-constrained B-cell epitope peptide. J Biol Chem 282:11436–11445

Olsen SN, Andersen KB, Randolph TW, Carpenter JF, Westh P (2009) Role of electrostatic repulsion on colloidal stability of Bacillus halmapalus alpha-amylase. Biochim Biophys Acta 1794:1058–1065

Parbhu A, Lin H, Thimm J, Lal R (2002) Imaging real-time aggregation of amyloid β protein (1-42) by atomic force microscopy. Peptides 23:1265–1270

Patel D, Henry J, Good T (2006) Attenuation of β-amyloid induced toxicity by sialic acid-conjugated dendrimeric polymers. Biochim Biophys Acta 1760:1802–1809

Pecora R (1985) Dynamic light scattering: application of photon correlation spectroscopy. Plenum, New York

Petkova AT, Leapman RD, Guo Z, Yau WM, Mattson MP, Tycko R (2005) Self-propagating, molecular-level polymorphism in Alzheimer's β-amyloid fibrils. Science 307:262–265

Russel WB, Saville DA, Showalter WR (1989) Colloidal dispersion. Cambridge University Press, Cambridge

Sahoo B, Nag S, Sengupta P, Maiti S (2009) On the stability of the soluble amyloid aggregates. Biophys J 97:1454–1460

Selkoe DJ (1999) Translating cell biology into therapeutic advances in Alzheimer's disease. Nature 399:A23–A31

Selkoe DJ (2004) Cell biology of protein misfolding: the examples of Alzheimer's and Parkinson's diseases. Nat Cell Biol 6:1054–1061

Shen C-L, Murphy RM (1995) Solvent effects on self-assembly of beta-amyloid peptide. Biophys J 69:640–651

Sicorello A, Torrassa S, Soldi G, Gianni S, Travaglini-Allocatelli C, Taddei N, Relini A, Chiti F (2009) Agitation and high ionic strength induce amyloidogenesis of a folded PDZ domain in native conditions. Biophys J 96:2289–2298

Stine BW Jr, Dahlgren KN, Krafft GA, LaDu MJ (2003) In vitro characterization of conditions for Amyloid-β Peptide oligomerization and fibrillogenesis. J Biol Chem 278:11612–11622

Tabner BJ, Turnbull S, El-Agnaf OMA, Allsop D (2001) Production of reactive oxygen species from aggregating proteins implicated in Alzheimer's Disease, Parkinson's Disease and other neurodegenerative diseases. Curr Top Med Chem 1:507–517

Talmard C, Bouzan A, Faller P (2007) Zinc binding to amyloid-β: isothermal titration calorimetry and Zn competition experiments with Zn sensors. Biochemistry 46:13658–13666

Taylor M, Moore S, Mayes J, Parkin E, Beeg M, Canovi M, Gobbi M, Mann DMA, Allsop D (2010) Development of a proteolytically stable retro-inverso peptide inhibitor of β-amyloid oligomerization as a potential novel treatment for Alzheimer's disease. Biochemistry 49:3261–3272

Weldon DT, Rogers SD, Ghilardi JR, Finke MP, Cleary JP, O'Hare E et al (1998) Fibrillar β-amyloid induces microglial phagocytosis, expression of inducible nitric oxide synthase, and loss of a select population of neurons in the rat CNS in vivo. J Neurosci 18:2161–2173

Yagi H, Ban T, Morigaki K, Naiki H, Goto Y (2007) Visualization and classification of amyloid β supramolecular assemblies. Biochemistry 46:15009–15017

Yan P, Hu X, Song H, Yin K, Bateman RJ et al (2006) Matrix metalloproteinase-9 degrades amyloid-β fibrils in vitro and compact plaques in situ. J Biol Chem 281:24566–24574

Yang Y-L, Kaufman LJ (2009) Rheology and confocal reflectance microscopy as probes of mechanical properties and structure during collagen and collagen/hyaluronan self-assembly. Biophys J 96:1566–1585

Zagorski MG, Yang J, Shao H, Ma K, Zeng HN, Hong A (1999) Methodological and chemical factors affecting amyloid β peptide amyloidogenicity. Method Enzymol 309:189–204

Zako T, Sakono M, Hashimoto N, Ihara M, Maeda M (2009) Bovine insulin filaments induced by reducing disulfide bonds show a different morphology, secondary structure, and cell toxicity from intact insulin amyloid fibrils. Biophys J 96:3331–3340